3rd URSI AT-AP-RASC, Gran Canaria, 29 May – 3 June 2022

Multi-line TRL Calibration for the Characterization of Transmission Media

Ana Buesa-Zubiria, and Jaime Esteban
The Information Processing and Telecommunications Center, Universidad Politécnica de Madrid, 28040 Madrid, Spain.

Abstract

The characterization of different transmission media has been carried out using the canonical polyadic decomposition formulation of the multi-line TRL calibration. Some improvements to this approach are presented. The measurement of microstrip lines from 500 MHz to 20.5 GHz has been carried out and the results discussed. Furthermore, a pseudo-SIW waveguide has also been characterized in the band from 4.5 to 7.5 GHz.

1 Introduction

The measurement of multiple lines differing only in length allows the characterization of transmission media as suggested by the procedure of the Multi-line Thru-Reflect-Line calibration (MTRL) [1–10]. The characterization of transmission media is becoming more and more important as the systems' frequency operation increases. Feed networks are becoming electrically large and, therefore, materials and transmission media that conforms them must be carefully characterized. In this communication, the recently published idea of a MTRL calibration using a tensor decomposition [11, 12] has been used to characterize different transmission media. Furthermore, some improvements to the implementation of the tensor decomposition method have been included. More precisely, the optimal Gauss-Markov formulation presented in [5–7] has been included in the derivation of the results.

Section 2 of this communication gives the main characteristics of, and details the improvements added to, the Canonical Polyadic Decomposition (CPD) in the multi-line calibration procedure. Then, Section 3 shows the results of a microstrip transmission medium characterization covering the 0.5 to 20.5 GHz frequency band, as well as the characterization of a pseudo-SIW waveguide from 4.5 to 7.5 GHz. Finally, some conclusions are presented in Section 4.

2 CPD Implementation Overview

If a set of N lines which do only differ in length is measured, the power-wave chain matrix $\mathbf{M}^i$ of the i-th measuremnent can be written as:

$$\mathbf{M}^i = \underbrace{\begin{bmatrix} x_{11} & x_{12} \\ x_{21} & x_{22} \end{bmatrix} A \begin{bmatrix} p & 0 \\ 0 & 1 \end{bmatrix} \mathbf{P}}_{\mathbf{X}} \mathbf{T}^i \underbrace{\mathbf{P} B \begin{bmatrix} q & 0 \\ 0 & 1 \end{bmatrix} \begin{bmatrix} y_{11} & y_{12} \\ y_{21} & y_{22} \end{bmatrix}}_{\mathbf{Y}} \tag{1}$$

where $\mathbf{T}^i$ is the chain matrix of the i-th line; $\mathbf{P}$ is a permutation matrix; A, p, B and q are unknown scalar values; and $\mathbf{X}$ and $\mathbf{Y}$ represent the VNA non-idealities. Then,

$$\begin{aligned} \mathbf{M}^i = ABpq \begin{bmatrix} x_{11}y_{11} & x_{11}y_{12} \\ x_{21}y_{11} & x_{21}y_{12} \end{bmatrix} e^{\mp\gamma l_i} + \\ AB \begin{bmatrix} x_{12}y_{21} & x_{12}y_{22} \\ x_{22}y_{21} & x_{22}y_{22} \end{bmatrix} e^{\pm\gamma l_i} \end{aligned} \tag{2}$$

which can be written as:

$$\begin{aligned} \mathbf{M}^i = \lambda_1 e^{\mp\gamma l_i} \begin{bmatrix} x_{11} \\ x_{21} \end{bmatrix} \begin{bmatrix} y_{11} & y_{12} \end{bmatrix} + \\ \lambda_2 e^{\pm\gamma l_i} \begin{bmatrix} x_{12} \\ x_{22} \end{bmatrix} \begin{bmatrix} y_{21} & y_{22} \end{bmatrix} \end{aligned} \tag{3}$$

or

$$\mathbf{M}^i = \lambda_1 e^{\mp\gamma l_i} \mathbf{a} \odot \mathbf{b} + \lambda_2 e^{\pm\gamma l_i} \mathbf{c} \odot \mathbf{d} \tag{4}$$

where $\odot$ denotes the outer product between two column vectors $\mathbf{a} \odot \mathbf{b} = \mathbf{a}\mathbf{b}^T$ being the superindex T the transpose operation. Hence, the external product of two vectors results in a matrix. Extending this definition to tensors, each new vector outer product adds a new dimension to the result. Then, we can write:

$$\mathscr{T} = \lambda_1 \mathbf{a} \odot \mathbf{b} \odot \mathbf{e}_1 + \lambda_2 \mathbf{c} \odot \mathbf{d} \odot \mathbf{e}_2 \tag{5}$$

where $\mathbf{e}_1$ and $\mathbf{e}_2$ contain the propagation factors of the N lines considered in the problem.

We can define the factor matrices:

$$\dot{\mathbf{X}} = \begin{bmatrix} \mathbf{a} & \mathbf{c} \end{bmatrix} = \begin{bmatrix} x_{11} & x_{12} \\ x_{21} & x_{22} \end{bmatrix} = \mathbf{X}\mathbf{P}\frac{1}{A} \begin{bmatrix} 1/p & 0 \\ 0 & 1 \end{bmatrix} \tag{6}$$

$$\dot{\mathbf{Y}}^T = \begin{bmatrix} \mathbf{b} & \mathbf{d} \end{bmatrix}^T = \begin{bmatrix} y_{11} & y_{12} \\ y_{21} & y_{22} \end{bmatrix} = \frac{1}{B} \begin{bmatrix} 1/q & 0 \\ 0 & 1 \end{bmatrix} \mathbf{P}\mathbf{Y} \tag{7}$$

and

$$\mathbf{D} = \begin{bmatrix} \mathbf{e}_1 & \mathbf{e}_2 \end{bmatrix} = \begin{bmatrix} e^{\mp\gamma l_1} & e^{\pm\gamma l_1} \\ e^{\mp\gamma l_2} & e^{\pm\gamma l_2} \\ \vdots & \vdots \\ e^{\mp\gamma l_N} & e^{\pm\gamma l_N} \end{bmatrix} \tag{8}$$

The **D** matrix is written this way to show that in each column of **D** we can obtain either a positive or a negative exponential, as a result of the presence of the permutation matrix **P**. But it is not possible that both types of exponentials are mixed in the same column, as it can be deduced from (4).

Then, with $\boldsymbol{\lambda} = \begin{bmatrix} \lambda_1 & \lambda_2 \end{bmatrix}$:

$$\mathscr{T} = [\boldsymbol{\lambda}; \dot{\mathbf{X}}, \dot{\mathbf{Y}}, \mathbf{D}] \tag{9}$$

which corresponds with the Canonical Polyadic Decomposition (CPD) operation. The CPD is a tensor decomposition that is unique, up to a permutation and scaling factors, when the sum of the factor matrices ranks, defined as the number of linearly independent columns, is greater or equal to $2F+2$ being F the number of summing elements in (4). So, in the MTRL calibration technique uniqueness is achieved. Therefore, if a tensor $\mathscr{T}$ containing the transmission parameters of N lines of different lengths, but with identical launchers, is formed, then the CPD leads to the matrices $\dot{\mathbf{X}}$, $\dot{\mathbf{Y}}$ and **D** in equations (6) to (8). The matrices **X** and **Y**, which define the VNA errors, can be obtained once the permutation **P** and the scaling factors are found.

2.1 CPD Solution

Note that the line order in (8) corresponds with the order in which the measured data is included in $\mathscr{T}$, since permutation **P** do not affect it. However, the numerical result of (9) for **D** matrix can include two arbitrary scale factors: one of them multiplies the entire matrix, the other multiplies one column and divides the other. Because of the exponential form of the matrix terms, this second factor can be interpreted as a change of the reference plane. Therefore, some information about the line lengths should be used to fully determine the **D** matrix. In [12] an optimization is carried out, whose results are both the scale factors and the estimation of γ. In the implementation described here the obtainment of the propagation constant has been separated from the deduction of the scale factors in order to use the Gauss-Markov results. Thus, it can be ensured that the best linear estimation of the propagation constant can be found, at least when only considering zero-mean additive white Gaussian noise (AWGN). Therefore, focusing throughout this section on the sole objective of determining the **D** matrix, a two-step normalization has been established. Firstly, just for simplicity and although it is not indispensable, the length of the line chosen as thru is set as zero. Then, each of the columns on (8) is normalized by the value on the position of the thru. This normalization gives special precedence to the accuracy of the result for the line chosen as thru. But the objective of the CPD is to make an approximation to the $\dot{\mathbf{X}}$, $\dot{\mathbf{Y}}$ and **D** values that best fit the tensor $\mathscr{T}$, without prioritizing any of the lines. This is why a second step has been included. The second step is based on an optimization, which finds the ξ factor that best fits that all the elements in $\mathbf{e_1}$, multiplied by their corresponding elements in $\mathbf{e_2}$, are equal to one. So, this second step can be seen as the fine-tuning of a factor ξ that must divide both columns in (8). The optimization problem is stated as:

$$\xi = \min_{v} \sum_{i=1}^{N} \left| \mathbf{e}_{i1}\mathbf{e}_{i2} - v^2 \right|^2 \tag{10}$$

where the summation includes the thru, and the sign of ξ is chosen so that the terms corresponding to the thru in the normalized **D** are close to $+1$ (and not to -1).

Furthermore, it is necessary to find the permutation that the CPD has introduced. An estimation of the propagation constant has been used in our implementation. The main reason for such a decision is that, when considering low-loss transmission lines and noise, there is no trivial way to clearly distinguish which is the positive exponential and which is the negative one in the rows of **D**.

The permutation **P** is found by minimizing the distance between the exponential terms of **D** and the exponentials calculated with an estimation of the propagation constant. One must be cautious not to take a line that is too short or too long to find the permutation. A short one increases the possibility to misidentify the exponential factors. But, if the line is too long, identification errors also arise because of the indetermination introduced by the periodicity of the phase.

2.2 Propagation Constant by CPD

Once the permutation is found, the values of the propagation constant are calculated at each frequency, as given by each of the elements in both columns of **D** (excluding those corresponding to the thru). The possible phase jumps are then removed (the phase is unwrapped) so that the resulting propagation constant is continuous with frequency. The propagation constants of the waves propagating in both directions are averaged to minimize the influence of second-order errors that may arise from differences between the connectors which allow to obtain $N-1$ propagation constants as

$$\gamma_{ij} = \frac{\ln\left(e^{+\gamma\Delta l_{ij}}\right) - \ln\left(e^{-\gamma\Delta l_{ij}}\right)}{2\Delta l_{ij}} \tag{11}$$

Then we have to calculate, again for each of the frequencies, the estimation of the propagation constant, $\hat{\gamma}$, combining the $N-1$ propagation constants γ_{ij} of (11). Their combination following the Gauss-Markov theorem is the main key of the multi-line algorithm. With it, it is possible to achieve the best unbiased linear estimation under a series of considerations about the nature of measurement errors.

Let's define $\mathbf{L}$, size $(N-1)\times 1$, as the array containing all the Δl_{ij} values and $\mathbf{G}$ as the size $(N-1)\times 1$ array with the $N-1$ values of γ_{ij}. If we name $\mathbf{V}$ of size $(N-1)\times(N-1)$ the measurement of the noise covariance we have that:

$$\hat{\gamma} = \frac{\mathbf{L}^H \mathbf{V}^{-1} \mathbf{G}}{\mathbf{L}^H \mathbf{V}^{-1} \mathbf{L}} \tag{12}$$

where the superindex H stands for hermitian transpose.

The calculation of the $\mathbf{V}$ matrix is another key element that was presented in [6]. Realizing that the eigenvalue solution uses the difference between two measurements ($\mathbf{M}^{ij}$), the noise covariance matrix must be filled in accordingly. Therefore, assuming that there is no correlation between the measurement of the different lines and that they are all equally noisy, we get:

$$\mathbf{V}^{-1} = \frac{1}{\sigma_k^2} \begin{bmatrix} 1-\frac{1}{N} & -\frac{1}{N} \\ -\frac{1}{N} & 1-\frac{1}{N} \end{bmatrix} \tag{13}$$

where σ_k is the variance of the noise in the individual line measurements, not being necessary its determination because of its appearance in the numerator as well as in the denominator of (12).

This approach is better than the optimization proposed and used in [12], since at least (12) provides the best linear estimator.

3 Measurements

3.1 Microstrip Transmission Medium

A multi-line microstrip calibration kit (see Fig. 1), consisting of nine lines and an open end, has been manufactured using 30-mil thick ARLON25N as substrate. The line lengths have been chosen to minimize the TRL calibration error in the range from 500 MHz to 20.5 GHz, namely, 40, 42.1, 44, 54.9, 69.4, 87.5, 97.3, 109 and 119.5 millimeters. The microstrip open end used as reflect has been located 20 mm away from the launcher. Thus, the use of the 40 mm line as a zero-length thru places the reflect in the reference plane of the measurements. However, the measurement of the reflect is not included here, since it is not needed for the characterization of the microstrip transmission medium.

The multi-line calibration kit in Fig. 1 has been measured with Southwest coaxial-to-microstrip launchers in an Agilent N5230A VNA, and the resulting S-parameters have been processed with Matlab.

The propagation constant, as extracted from the measurements, is shown in Fig. 2. Its real part, the attenuation constant, is the most sensitive parameter and it can be seen how

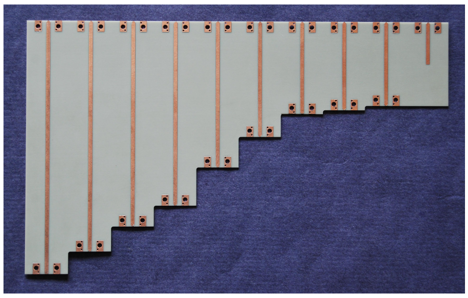

Figure 1. Manufactured multi-line TRL calibration kit

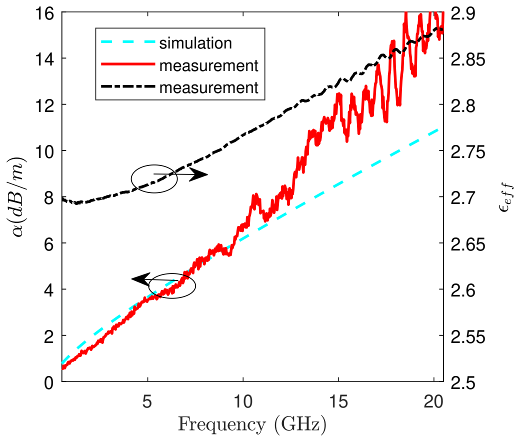

Figure 2. Attenuation constant and effective relative permittivity for the measured microstrip transmission medium.

above 10 GHz a little ripple appears in this parameter. Authors associate this ripple to the connectors frequency response deterioration with frequency. The simulated attenuation constant, from a quasi-TEM approximation, has been included in Fig. 2 for comparison. Finally, the effective relative permittivity is also shown in Fig. 2, which completes the characterization of the manufactured microstrip.

3.2 Pseudo-SIW

In order to show the potential of this procedure for the characterization of all kind of transmission media, an air-filled pseudo-SIW waveguide has been manufactured, see Fig. 3. This structure is not exactly a SIW waveguide, since posts are not close enough to make the waveguide behave as a closed medium. Therefore, the measurement of this waveguide, and its resulting attenuation constant, is going to take into account radiation losses.

A number of line lengths have been chosen to minimize the TRL uncertainties in the range from 4.5 GHz to 7.5 GHz leading to: 63, 84, 105, 126, 189, 210, 273, 357, 399 and 441 mm. The shortest has been considered as thru. Furthermore, 3.5 mm coaxial ports have been used as launchers. The measurement has also been carried out with an Agilent N5230A VNA, and the resulting S-parameters pro-

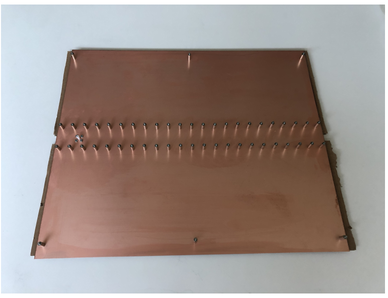

Figure 3. Manufactured pseudo-SIW waveguide.

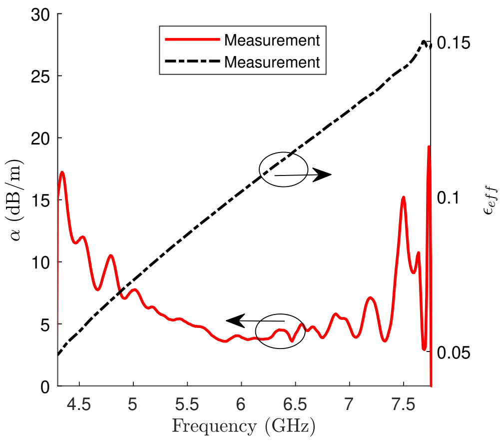

Figure 4. Attenuation constant and effective relative permittivity for the measured pseudo-SIW waveguide.

cessed with Matlab.

The real part of the propagation constant together with the relative permittivity of the pseudo-SIW waveguide is shown in Fig. 4 and they agree with the results presented in [13], obtained by a different and much more laborious procedure.

4 Conclusions

Through the rigorous completion of the MTRL calibration technique by tensor decomposition, the characterization of any transmission medium is possible without no more than manufacturing several lines which do only differ in length. Along this communication improvements in the implementation of the MTRL by means of the CPD have been included, which implies that more accurate characterizations are now possible. A microstrip line as well as a pseudo-SIW waveguide had been measured and results are satisfactory.

5 Acknowledgements

This work was supported by the Spanish Government under Grant PID2020-116968RB-C33 (DEWICOM) funded by MCIN/AEI/10.13039/501100011033 (Agencia Estatal de Investigación) and by the European Space Agency under contract 4000135255/21/NL/GLC/my.

References

[1] H. V. Shurmer, "Calibration procedure for computer-corrected S parameter characterisation of devices mounted in microstrip," *Electron. Lett.*, vol. 9, no. 14, pp. 323–324, Jul. 1973.

[2] S. Rehnmark, "On the calibration process of automatic network analyzer systems (short papers)," *IEEE Trans. Microw. Theory Techn.*, vol. 22, no. 4, pp. 457–458, Apr. 1974.

[3] G. F. Engen and C. A. Hoer, "Thru-reflect-line: An improved technique for calibrating the dual six-port automatic network analyzer," *IEEE Trans. Microw. Theory Techn.*, vol. 27, no. 12, pp. 987–993, Dec. 1979.

[4] C. A. Hoer and G. F. Engen, "On-line accuracy assessment for the dual six-port ANA: Extension to nonmating connectors," *IEEE Trans. Instrum. Meas.*, vol. IM-36, no. 2, pp. 524–529, Jun. 1987.

[5] R. B. Marks, "Multi-line calibration for MMIC measurement," in *36th ARFTG Conf. Dig.*, vol. 18, Nov. 1990, pp. 47–56.

[6] ——, "A multiline method of network analyzer calibration," *IEEE Trans. Microw. Theory Techn.*, vol. 39, no. 7, pp. 1205–1215, Jul. 1991.

[7] D. C. DeGroot, J. A. Jargon, and R. B. Marks, "Multiline TRL revealed," in *60th ARFTG Conf. Dig.*, Dec. 2002, pp. 131–155.

[8] H.-J. Eul and B. Schiek, "A generalized theory and new calibration procedures for network analyzer self-calibration," *IEEE Trans. Microw. Theory Techn.*, vol. 39, no. 4, pp. 724–731, Apr. 1991.

[9] A. Ferrero and U. Pisani, "Two-port network analyzer calibration using an unknown 'thru'," *IEEE Microw. Guided Wave Lett.*, vol. 2, no. 12, pp. 505–507, Dec. 1992.

[10] D. F. Williams and R. B. Marks, "LRM probe-tip calibrations using nonideal standards," *IEEE Trans. Microw. Theory Techn.*, vol. 43, no. 2, pp. 466–469, Feb. 1995.

[11] Y. Rolain, M. Ishteva, E. Van Nechel, and F. Ferranti, "Multi-line TRL revisited," in *85th Microw. Meas. Conf. (ARFTG)*, May. 2015, pp. 1–3.

[12] ——, "A tensor-based extension for the multi-line TRL calibration," *IEEE Trans. Microw. Theory Techn.*, vol. 64, no. 7, pp. 2121–2128, Jul. 2016.

[13] J. E. Varela and J. Esteban, "Analysis of laterally open periodic waveguides by means of a generalized transverse resonance approach," *IEEE Transactions on Microwave Theory and Techniques*, vol. 59, no. 4, pp. 816–826, 2011.